Microreactors

DOI: 10.1002/ange.200805933

Synthesis of Goethite by Separation of the Nucleation and Growth Processes of Ferrihydrite Nanoparticles Using Microfluidics**

Ali Abou-Hassan, Olivier Sandre, Sophie Neveu, and Valérie Cabuil*

Continuous-flow and droplet-based microreactors have been widely used for studying and optimizing chemical reactions.[1–13] Nanoparticles, such as CdS[5] and CdSe[6] quantum dots, CdSe–ZnS core–shell structures,[7] metallic Pd, Co, Ag, and Au,[8] γ-Fe_2O_3,[9,10] SiO_2,[11] TiO_2,[12] and SiO_2–TiO_2 core–shell structures have been synthesized using microfluidic devices.[13] Compared to conventional bulk synthesis, microfluidics offers a better control of the reaction parameters, such as temperature and mass transfer, which can lead to a better control of the particle sizes.[1–4] Goethite (α-FeOOH) is an iron oxyhydroxide that is widely found in iron-rich soils.[14] This clay mineral constitutes the natural ochre pigment, and because of its elongated shape, synthetic goethite is often used as a precursor of α-Fe "hard magnet" particles for magnetic recording.[15] Because of this elongated shape, suspensions of antiferromagnetic goethite/plate-like nanostructures (nanolaths) exhibit an original magneto-optical effect, and self-assemble spontaneously into a nematic liquid-crystal phase above a threshold concentration.[16] Different methods have been reported for the synthesis of acicular (needle-like) goethite particles based on aging of the ferrihydrite nanoparticles obtained by alkalinization of iron(III) salt solutions.[17] However, a microfluidic synthesis of goethite particles has not been demonstrated to date. The importance of particle shape for the improvement of magnetic properties, or the control of the particle assembly, requires control of the synthetic conditions of these particles. [18,19]

"Digital microfluidics," which tunes the biphasic flows, is a very popular method to produce microdroplets that behave as microreactors for the synthesis of nanoparticles. However, this method frequently uses oils and surfactants that can affect the nucleation–growth mechanisms of the particles. Compared to microdroplet reactors, continuous-flow reactors are easier to handle and are more representative of the conditions of the bulk synthesis, with improved homogeneity, thus offering a better reproducibility of the particles synthesized.[20] Another benefit provided by the continuous microfluidic systems is the ability to add reagents along the entire length of the channel without the need to synchronize with a dropping frequency that is required for microdroplets reactors.[21] Mixing various chemical species in the continuous-flow reactor is diffusion-limited at the confluence of the flows.[22] To overcome this limitation, hydrodynamic flow focusing has been envisioned, which is based on constriction of a sample flow between sheath flows by using appropriate geometrical conditions. This method reliably reduces the diffusion lengths and decrease the mixing times.[23] By adjusting the volumetric rates of the sample and sheath flows respectively, a stable central jet is achieved. Furthermore, the parabolic velocity profile due to the laminar Poiseuille flow is nearly flat at the center of the focalized jet flow and can be described as a plug flow, which ensures minimization of the shear stress that causes the Taylor–Aris dispersion effect. This effect is usually observed during the nanoparticles synthesis as the chemical reaction proceeds in the sample jet.[24]

Herein we describe a new method based on microfluidics that allows the acceleration and the control of the production of small goethite nanolaths. The idea is to physically separate the process of nucleation of the ferrihydrite nanoparticles from their growth, thus leading to goethite particles. The nucleation of the primary ferrihydrite nanoparticles is induced by diffusive mixing at room temperature in a microreactor that is based on a coaxial flow geometry (R1; Figure 1). This mixing reactor[9] is based on a three-dimensional coaxial-flow device of two streaming reagents. The 3D hydrodynamic geometry allows a rapid homogeneity of the reactants through focalization, and avoids technical barriers,

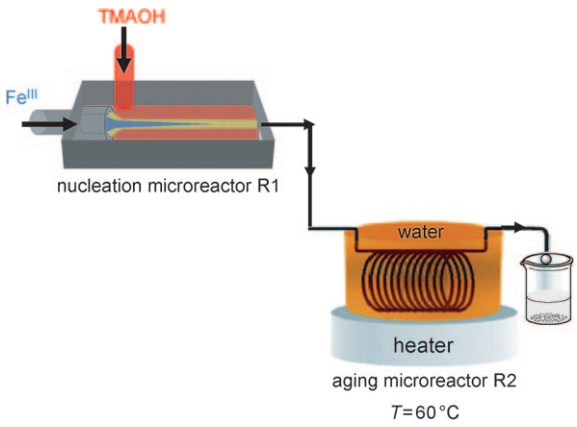

Figure 1. The experimental setup used for the preparation of the ferrihydrite and goethite nanoparticles. TMAOH = tetramethylammonium hydroxide.

[*] Dr. A. Abou-Hassan, Dr. O. Sandre, Dr. S. Neveu, Prof. V. Cabuil
UPMC Univ Paris 6, Laboratoire des Liquides Ioniques et Interfaces Chargées UMR 7612, équipe Colloïdes Inorganiques (LI2C), Université Paris 6 (UPMC) Bat F(74), case 51
4 place Jussieu, 75252 Paris Cedex 05 (France)
Fax: (+33) 1-4427-3675
E-mail: ali.abou_hassan@upmc.fr
Homepage: http://www.li2c.upmc.fr

[**] We thank Patricia Beaunier from the Electron Microscopy Facility (UPMC, UFR 926) for the TEM and HRTEM images, Virginie Georget from the cellular imaging facility for the LCSM images (UPMC, IFR 83), and Preston Mohr and Thomas Boudier (UPMC, IFR 83) for fruitful discussions regarding image analysis.

such as channel clogging and precipitation of the chemical species along the reactor walls.

To induce the nucleation reaction in the R1 microreactor, the iron (III) chloride solution in hydrochloric acid, and the alkaline solution of tetramethylammonium hydroxide (TMAOH) were flushed into the inner and the outer streams, respectively, with the rate flows of Q_{in} and Q_{out}. The rate flow of the different species can be continuously adjusted to produce a stable inner stream and different mixing times. Fast mixing is required to ensure a homogeneous and uniform chemical composition of the nucleation region in the microreactor.

The mixing time is determined experimentally from a 3D mapping of pH inside the channel R1; a detailed physical analysis, including numerical simulations, will be published elsewhere. In a first approximation, mixing time by flow focusing in the laminar regime is independent of the total volumetric flow rate Q_{tot} and depends only on the ratio of the outer to inner flow rates Q_{out}/Q_{in}.[25] However, our preliminary results indicate that increasing Q_{tot} also has a strong effect on the polydispersity of the produced nanoparticles by decreasing the width of the residence time distribution. Experimentally, the quantitative analysis of the mixing time and the pH mapping in the nucleation reactor R1 were performed by labeling the acidic inner stream by a 6 μM fluorescein solution. Fluorescein is used as a pH probe as it can exist in several ionization forms, each having distinct spectral properties.[26] Figure 2 shows the fluorescence intensity versus pH curve for

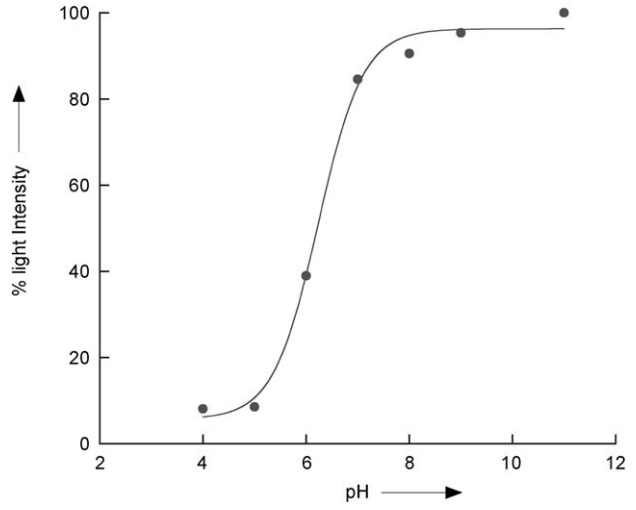

Figure 2. Fluorescence intensity of a fluorescein solution (6 μM) at different pH values.

6 μM solution of fluorescein. Following the fluorescein emission intensity inside the mixing channel R1 using confocal laser scanning microscopy (CLSM), we obtain a cross-section plot of the pH change along the focused stream jet, and were able to estimate the mixing time by assuming a linear relationship between time and position. The best mixing time achieved in the micromixer R1 is about 80 ms for the ratio $Q_{out}/Q_{in} \approx 400$.

Figure 3 shows the dynamic mixing in the focused jet owing to diffusion of the hydroxide ions flowing in the outer stream into the fluorescein central stream. The fast mixing is inferred from the sudden increase of the fluorescence

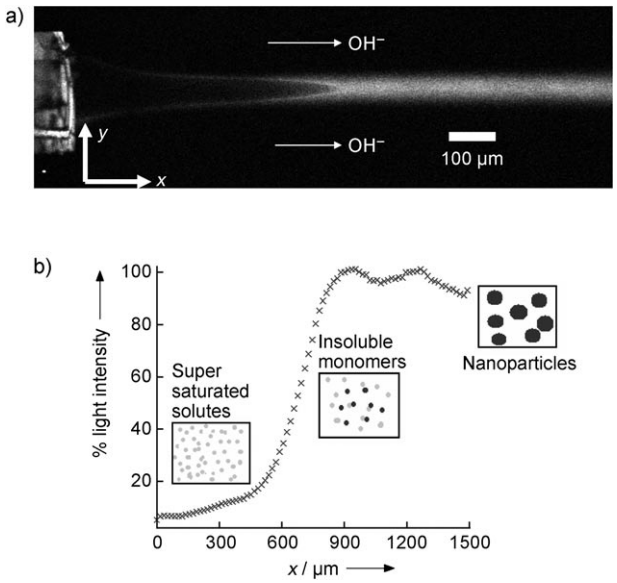

Figure 3. a) CLSM image during the mixing of the acidic inner stream labelled with fluorescein (6 μM) solution with the outer stream of TMAOH solution. The flow rates are $Q_{in} = 0.5\ \mu L\,min^{-1}$ and Q_{out} 200 $\mu L\,min^{-1}$. b) Average plot profile of the fluorescence intensity in the inner stream, as a function of position in the channel during mixing, which reflects the pH variation.

intensity of fluorescein over a pH range of two units around a pH of about 6.2, before reaching a plateau for a pH value of about 13 (owing to the final concentration of TMAOH). As the pH rises above 7, the solubility of the iron(III) species decreases, and as soon as the supersaturation concentration is reached, nucleation of ferrihydrite occurs.

Before aging, a drop is collected at the outlet of reactor R1 and analyzed using TEM. Figure 4a shows well-defined spherical ferrihydrite nanoparticles (nanodots) of about 4 ± 1 nm in size. The electron diffraction pattern of a large selected zone confirms the presence of poorly crystalline

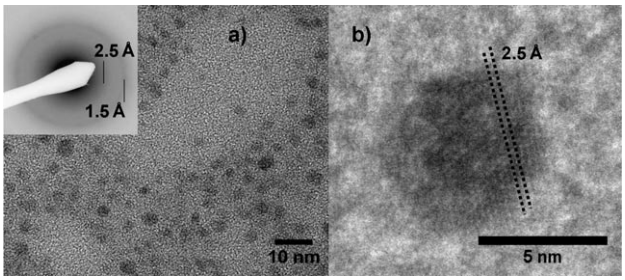

Figure 4. a) TEM picture of the sample taken after precipitation in the microreactor R1 (before aging), showing ferrihydrite nuclei of 4 ± 1 nm diameter. The selected area-diffraction pattern (inset) is typical of two line ferrihydrite. b) HRTEM image of an individual ferrihydrite nanoparticle with a 2.5 Å lattice fringe.

ferrihydrite, as indicated by two diffused diffraction rings.[17] High-resolution TEM (HRTEM) measurements (Figure 4b) show that the nanoparticles are monocrystalline, exhibiting atomic planes with an interplanar distance of about 2.5 Å, which is consistent with ferrihydrite nanoparticles.

At the outlet of the micromixer R1, the suspended ferrihydrite nanoparticles are directly injected into the microtubular aging coil R2 ($L = 150$ cm), which is continuously heated in a water bath at 60 °C. Temperature profiles are calculated to determine the tubing length (and thus the time) required for the fluid to reach a steady state. Under the given flow rate, the ferrihydrite solution reaches 60 °C in about 1 s, that is, within the first centimeter after it has entered the heated zone of the tubing. The effective residence time is about 15 min, as estimated from the length of the tubing along which the fluid has reached the stationary temperature of 60 °C.

After aging for 15 min under continuous flow through aging coil R2, goethite plate-like nanostructures were observed with an average length $L = 30 \pm 17$ nm and width $w = 7 \pm 4$ nm ($N = 100$ particles), yielding an axial ratio (L/w) of 4 ± 4 (Figure 5a). This short aging time appeared to be sufficient for the growth of crystalline and anisotropic goethite nanoparticles that differ only in smaller sizes

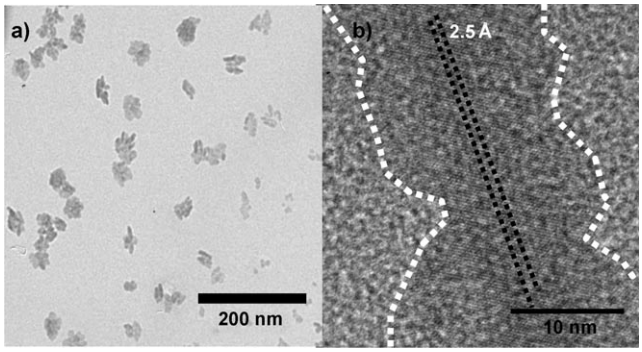

Figure 5. a) TEM image of the nanolaths after aging for 15 min in the microtubular loop R2, produced at pH 13 and under laminar flow. b) HRTEM image of a nanorod particle. Lattice fringe spacing is consistent with goethite. The dashed lines serve to highlight the morphology and texture of the particle.

compared to those obtained after complete aging (one day at 60 °C).[27] Moreover, the presence of remaining ferrihydrite nuclei undergoing aggregation in the batch after 15 min and even after 24 h at 60 °C (data not shown) supports the idea that goethite nanoparticles were formed by the aggregation mechanism rather than by dissolution/reprecipitation. We attribute (040) indexes to the lattice fringes with 2.5 Å spacing, which runs parallel to the length of the crystal (thereby an evidence of monocrystallinity) as imaged by HRTEM (Figure 5b). In addition, this crystal of appears to be composed of nodules that are similar in size to the nanodots, which is consistent with the idea that growth proceeds by aggregation of nuclei that are aligned by the shear stress of the laminar flow.

In summary, we have demonstrated a significant acceleration of the synthesis of goethite nanoparticles from ferrihydrite nuclei by the use of a continuous-flow microfluidic system. The novelty of this approach lies in the separation of the nucleation of the primary particles (ferrihydrite) and growth of the goethite nanoparticles in two independent microreactors operating in different conditions. In the nucleation microreactor, the streaming reagents are mixed by molecular diffusion at room temperature in a flow-focusing geometry. The homogeneity of the mixture is ensured by the fast mixing time that is estimated by fluorescence microscopy. Furthermore, the technical difficulty of microchannel clogging owing to precipitation onto the walls is avoided by the 3D geometry. Bulk synthesis usually yields goethite nanoparticles with a typical length of about 250 nm and width of 40 nm, with a polydispersity index of about 50% for both dimensions.[28] Our method in a microfluidic aging channel minimizes local temperature gradients, ensures a regular laminar flow, and finally leads to crystalline plate-like nanostructures. These particles have approximately the same values of aspect ratio and polydispersity index obtained in the bulk synthesis, but are smaller in size. The time required for aging presented herein (15 min for a velocity of 0.1 cm s^{-1}) compared to bulk synthesis (several hours or days) may originate from the small diameter of the aging reactor, causing a shear stress that prealigns the primary ferrihydrite nanoparticles and speeds up their oriented aggregation process. Apart from the importance of the different applications of goethite, this work opens up a new area for the use of microfluidics in the aging process of materials dispersed in a fluid carrier.

Experimental Section

The coaxial flow micromixer (R1) is obtained by molding in poly(dimethylsiloxane) (PDMS) and is described in details in reference [9]. The aging microtubular loop (R2) consists of a transparent PTFE tube of 1.7 mm inner diameter and 150 cm total length (Upchurch Scientific). Harvard Apparatus syringe pumps (pico 11 plus) were used to control the flow rates. As starting materials for the precipitation of iron oxyhydroxide nanoparticles, we used analytical grades of $FeCl_3$ (27%, VWR), tetramethylammonium hydroxide (TMAOH; 97%, Sigma Aldrich), and hydrochloric acid HCl (37%, VWR). For the CLSM images, fluorescein sodium salt $C_{20}H_{10}Na_2O_5$ (98.5%, Sigma Aldrich) was used. 0.1M and 0.01M Fe(III) solutions are prepared by dilution of the commercial solution by 0.1M HCl solution. Freshly prepared TMAOH solution (0.1M, pH 13) was used so that carbonation of the solution doesn't occur. Fluorescein sodium salt solution (6 μm) is prepared by adding fluorescein sodium salt to hydrochloric acid (0.1M). TEM and HRTEM images were recorded with a JEOL JEM 100CX transmission electron microscope operating at 100 kV with a point to point resolution of 0.3 nm. Confocal laser scanning microscopy (CLSM) was performed on a Leica SP5 microscope with a 5X (O.11NA) objective. The 488 nm argon laser line was used for excitation, and emitted fluorescence spectra were collected between 500 and 600 nm.

Received: December 5, 2008
Published online: February 16, 2009

Keywords: goethite · microfluidics · microreactors · nanoparticles · nucleation and growth

[1] W. Ehrfeld, V. Hessel, H. Lowe, *Microreactors: New Technology for Modern Chemistry*, Wiley-VCH, Weinheim, **2000**.
[2] K. Jähnisch, V. Hessel, H. Löwe, M. Baerns, *Angew. Chem.* **2004**, *116*, 410 – 451; *Angew. Chem. Int. Ed.* **2004**, *43*, 406 – 446.
[3] K. F. Jensen, *Chem. Eng. Sci.* **2001**, *56*, 293 – 303.
[4] A. J. deMello, J. C. deMello, *Lab Chip* **2004**, *4*, 11N – 15N.
[5] J. B. Edel, R. Fortt, J. C. deMello, A. J. deMello, *Chem. Commun.* **2002**, 1136 – 1137.
[6] B. K. H. Yen, A. Günther, M. A. Schmidt, K. F. Jensen, M. G. Bawendi, *Angew. Chem.* **2005**, *117*, 5583 – 5587; *Angew. Chem. Int. Ed.* **2005**, *44*, 5447 – 5451.
[7] H. Wang, X. Li, M. Uehara, Y. Yamaguchi, H. Nakamura, M. Miyazaki, H. Shimizu, H. Maeda, *Chem. Commun.* **2004**, 48 – 49.
[8] D. Shalom, R. C. R. Wootton, R. F. Winkle, B. F. Cottam, R. Vilar, A. J. deMello, C. P. Wilde, *Mater. Lett.* **2007**, *61*, 1146 – 1150.
[9] A. Abou Hassan, O. Sandre, V. Cabuil, P. Tabeling, *Chem. Commun.* **2008**, 1783 – 1785.
[10] L. Frenz, A. El Harrak, M. Pauly, S. Bégin-Colin, Andrew D. Griffiths, J.-C. Baret, *Angew. Chem.* **2008**, *120*, 6923 – 6926; *Angew. Chem. Int. Ed.* **2008**, *47*, 6817 – 6820.
[11] S. A. Khan, A. Gunther, M. A. Schmidt, K. F. Jensen, *Langmuir* **2004**, *20*, 8604 – 8611.
[12] B. F. Cottam, S. Krishnadasan, A. J. DeMello, J. C. DeMello, M. S. P. Shaffer, *Lab Chip* **2007**, *7*, 167 – 169.
[13] S. A. Khan, K. F. Jensen, *Adv. Mater.* **2007**, *19*, 2556 – 2560.
[14] J. F. Banfield, S. A. Welch, H. Zhang, T. T. Ebert, R. L. Penn, *Science* **2000**, *289*, 751 – 754.
[15] N. O. Nuñez, M. P. Morales, P. Tartaj, C. J. Serna, *J. Mater. Chem.* **2000**, *10*, 2561 – 2565.
[16] G. J. Vroege, D. M. E. Thies-Weesie, A. V. Petukhov, B. J. Lemaire, P. Davidson, *Adv. Mater.* **2006**, *18*, 2565 – 2568.
[17] U. Schwertmann, E. Murad, *Clays Clay Miner.* **1983**, *31*, 277 – 292.
[18] M. P. Sharrock, R. E. Bodnar, *J. Appl. Phys.* **1985**, *57*, 3919 – 3924.
[19] B. J. Lemaire, P. Davidson, J. Ferré, J. P. Jamet, D. Petermann, P. Panine, I. Dozov, J. P. Jolivet, *Eur. Phys. J. E* **2004**, *13*, 291 – 308.
[20] A. Jahn, J. Reiner, W. Vreeland, D. DeVoe, L. Locascio, M. Gaitan, *J. Nanopart. Res.* **2008**, *10*, 925 – 934.
[21] C.-H. Chang, B. Paul, V. Remcho, S. Atre, J. Hutchison, *J. Nanopart. Res.* **2008**, *10*, 965 – 980.
[22] Y. Song, J. Hormes, C. S. S. R. Kumar, *Small* **2008**, *4*, 698 – 711.
[23] J. B. Knight, A. Vishwanath, J. P. Brody, R. H. Austin, *Phys. Rev. Lett.* **1998**, *80*, 3863 – 3866.
[24] a) O. Levenspiel, *Chemical Reaction Engineering*, 3rd ed., Wiley, New York, **1999**; b) C. A. Silebi, J. G. Dosramos, *AIChE J.* **1989**, *35*, 1351 – 1364.
[25] L. D. Scampavia, G. Blankenstein, J. Ruzicka, G. D. Christian, *Anal. Chem.* **1995**, *67*, 2743 – 2749.
[26] D. Margulies, G. Melman, A. Shanzer, *Nat. Mater.* **2005**, *4*, 768 – 771.
[27] S. Krehula, S. Popovic, S. Music, *Mater. Lett.* **2002**, *54*, 108 – 113.
[28] D. M. E. Thies-Weesie, J. P. de Hoog, M. H. Hernandez Mendiola, A. V. Petukhov, G. J. Vroege, *Chem. Mater.* **2007**, *19*, 5538 – 5546.

